Extrusion Suppression of TSV Filling Metal by Cu-W Electroplating for Three-Dimensional Microelectronic Packaging

MYONG-HOON ROH, ASHUTOSH SHARMA, JUN-HYEONG LEE, and JAE-PIL JUNG

Extrusion behavior of Cu filling in through-silicon-via (TSV) under thermal loading was investigated in this study. In order to suppress the extrusion of Cu-filled TSV, Cu-W was filled in a tapered TSV by electroplating. The Cu-filled TSV was used as a reference for comparison. Defect less filling of Cu-W in TSV was achieved at a composition 92.4 wt pct Cu and 7.6 wt pct W. The coefficients of thermal expansion of both Cu-7.6 pctW and Cu were 10.8×10^{-6}/°C and 16.5×10^{-6}/°C, respectively. Initially, both Cu and Cu-W filled TSVs were annealed for 30 minutes at 723 K (450 °C) and the extrusion heights were measured. The results showed that the extrusion of Cu-W filled was suppressed significantly compared to Cu-filled TSVs. The annealed extrusion heights of Cu and Cu-W were found to be 1.369 and 0.465 μm, respectively. This showed around 34 pct lower extrusion height of Cu-W filled TSV as compared to Cu-filled TSV. The extrusion kinetics with different annealing durations and the mechanism of the suppression of extrusion in Cu-W filled TSV are also reported here.

DOI: 10.1007/s11661-015-2801-z
© The Minerals, Metals & Materials Society and ASM International 2015

I. INTRODUCTION

TSV is an attractive core technology for three-dimensional (3D) integration and packaging due to its various advantages such as short vertical interconnection, reduction in packaging volume, low power consumption, and multi-functionality.[1–3] TSV technologies are mainly studied for the micro-fabrication processes such as method of *via* formation, functional layers, *via* filling, wafer thinning, and stacking.[4–8] Although TSV is an advanced technology which is capable of maintaining 'Moore's Law' in semiconductor integration, yet reliability and cost are still major concerns for the practical application of the product.[9–11] The major reliability problems in TSV technology include extrusion, crack, and delamination of the Cu-filled TSV which are usually caused by the mismatch of CTE between surrounding Si substrate and TSV filling metal.[12–14] Enormous amount of research activities have been performed in the past to overcome these reliability problems.[15–17] For instance, in order to suppress the Cu extrusion, Tsai *et al*. added the pre-chemical mechanical polishing (CMP) step in the middle of back end of line (BEOL) processes.[15] They carried out pre-CMP at 623 K (350 °C), and succeeded in suppressing the Cu extrusion up to 50 nm at 673 K (400 °C). However, additional Cu-extruded region was detected in the subsequent Cu line capping layer deposition step. In other study, Ryu *et al*. calculated the stress distribution on the wafer, and located the devices in a position without stress called keep-away zone.[17] However, this method may cause the problem of low integration in semiconductor chips. There are various reports on the TSV filling to improve the performance and reliability, such as Cu-filled TSV with nanotwin structures.[18–21] The formation mechanism of these nanotwins is not clear which makes it difficult to control their population for large scale production.[22] Carbon nanotubes (CNTs) have also been investigated as a TSV filling material in the past. However, specialized techniques are required for CNT growth inside TSV.[23,24] Moreover, the co-plating of CNTs requires their uniform distribution inside the copper matrix which is sometimes difficult to control. In few reports, polymer filling of the TSVs has also been examined. However, there are problems of shrinkage or partial filling and polymer may degrade over time.[25,26] Recently, SiC-based and Bi-Sn-Ag solders have been tested for the TSV filling. However, extrusion properties are not discussed.[5,27]

Therefore, it is necessary to find a fundamental solution to suppress the extrusion of Cu-filled TSVs. One of the direct methods for suppressing Cu extrusion in TSVs involves the minimization of the difference of CTE between silicon (or insulating layer) and Cu layer. The CTE of Cu layer cannot be changed because it is a unique property of the material. The CTE difference can only be minimized by alloying copper with metals having lower CTE values such as W, Cr, and Mo. The CTE of W (~4.5×10^{-6}/°C) is 1.7 times greater than that of Si (2.6×10^{-6}/°C), while the CTE of pure Cu is 16.5×10^{-6}/°C. Thus, Cu-W layer will show a smaller CTE mismatch to Si as compared to the same with Cu

MYONG-HOON ROH, formerly with the Department of Materials Science and Engineering, University of Seoul, Seoul 130-743, South Korea, is now Specially Appointed Researcher with the Joining and Welding Research Institute (JWRI), Osaka University, 11-1 Mihogaoka, Ibaraki, Osaka 567-0047, Japan. ASHUTOSH SHARMA, Research Professor, JUN-HYEONG LEE, Master Grade, and JAE-PIL JUNG, Professor, are with the Department of Materials Science and Engineering, University of Seoul. Contact e-mail: jpjung@uos.ac.kr

Manuscript submitted June 23, 2014.
Article published online February 18, 2015

layer.[28] In addition, W has been considered as a conductive material that can replace Cu in TSV due to its good electrical conductivity of the order of metals like Cu and Au. W has already been used as a functional layer in the TSV. W has been applied for filling TSVs with smaller *via*, *e.g.*, less than 1 μm using chemical vapor deposition (CVD).[29] However, due to high melting point and extremely high hardness of W, the post-treatment process after *via* filling becomes highly expensive. Generally, Cu-W alloy is fabricated by spark plasma sintering (SPS) and melt-infiltration with the application of high pressure.[30,31] Such methods are not feasible in the 3D packaging including TSV. Thus, Cu-W alloy must be manufactured using an appropriate method.

Electroplating is a representative process for Cu filling in TSV which is relatively less expensive and have ease of mass production. W containing alloys such as Ni-W, Ni-Cr-W, and Co-W have been partially studied as a barrier layer to suppress Cu diffusion in coatings.[32–35] However, there is a limiting research activity on the synthesis of Cu-W or W by electroplating. In this study, Cu-W alloy was selected for TSV filling due to its combined features of both Cu and W. Cu-W alloy was electroplated to suppress extrusion of filling material in this study. Cu and Cu-W was filled in TSV with a tapered *via* by electroplating, and extrusion behavior of Cu and Cu-W was comparatively analyzed.

II. EXPERIMENTAL PROCEDURE

A. *Via Formation*

A p-type (100) single-crystal Si wafer with diameter of 100 mm and thickness of 525 μm was used as a substrate. Dry photoresists were employed for the fabrication of tapered vias in the silicon wafer. After the formation of pattern, tapered *via* was created with entrance diameter of 44 μm, bottom diameter of 34 μm, and *via* depth of 60 μm, respectively using deep reactive ion etching (DRIE) method.[36] The inclination angle of tapered *via* was 11 deg. About 1 μm thick insulating layer of SiO_2 was deposited on *via* walls using high density plasma chemical vapor deposition (HDPCVD). Ti and Cu depositions were followed as an adhesion and a seed layer, respectively, using a sputter coater. The as-fabricated cross section SEM image of TSV with a tapered *via* is shown in Figure 1.

B. *Plating Bath Formulation*

The electrolytic bath for Cu-W alloy was composed of sulfuric acid (H_2SO_4): 0.15 mol/L, copper sulfate ($CuSO_4 \cdot 5H_2O$): 0.05 mol/L, and W salt ($Na_2WO_4 \cdot 2H_2O$): 0.05 to 0.2 mol/L. Thriethanolamine (TEA): 0.3 mol/L was added as a complexing agent. There were two additives in the plating bath: polyethylene glycol (PEG, molecular weight 8000 g/mol) ~10 mg/L as a suppressor, and bis(sodiumsulfopropyl)disulfide (SPS): 3 mg/L as an accelerator/brightening agent. The complexing agents are generally reported to shift the

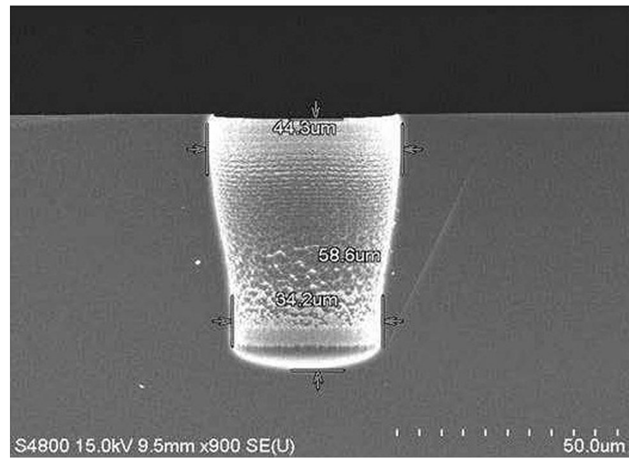

Fig. 1—Cross-section SEM image of as-fabricated tapered TSV.

equilibrium potentials to more negative values, and facilitate the co-deposition of metals with a wide range of over potential gaps.[37] The role of TEA as the complexing agent has been previously reported in Ni-W and Cu plating baths.[38,39] If added in small amounts, the complexing agents increase the plating rate of the co-deposition and further prevent the co-precipitation of the metal salts thereby suppressing the tendency of dendritic growth. The suppressor prevents the growth of metal ions at the *via* entrance, while accelerator increases the metal growth rate at the bottom of the *via* leading to a bottom up-filling.[40] This competition between accelerator and suppressor produces a void free and complete TSV filling. A magnetic bar was used for electrolyte stirring at 200 rpm. Prior to electrodeposition, the plating bath was maintained at room temperature 301 K (~28 °C), for a duration of 24 hours.

C. *Via Filling Through Pulse Periodic Reverse (PPR) Electroplating*

PPR electroplating was performed for Cu-W filling in a tapered *via* at room temperature. Pure Cu was also filled in a same sized *via* as reference. A commercial pulse plating unit (EPP4000, Princeton Applied Research Co.) was used to supply plating current. The plating cell was composed of three electrode geometry. A platinum plate (purity, 99.9 pct) was selected as an anode, and a saturated calomel electrode (SCE) was used as a reference electrode. PPR waveform was utilized for electroplating inside TSVs. The use of PPR waveform is beneficial for reducing defects in electroplated coatings.[41,42] It consists of cathodic cycle, anodic cycle and a current-off cycle (Figure 2). The deposition occurs during cathodic cycle, and the protruded regions due to the over deposition at *via* entrance are leveled off in anodic cycle. A high concentration of Cu ions that builds up during anodic cycle around *via* entrance is diminished during current-off cycle. The cathodic current density of PPR waveform for Cu and Cu-W filling were -2.624 and -0.875 mA/cm^2, respectively.

D. *Extrusion Behavior*

The top down surfaces of Cu and Cu-W filled TSVs were prepared by mechanical polishing with SiC papers (Grit #1200 and #2400) according to ASTM E-3 95 standard. Ultrasonic cleaning was performed on TSVs further to remove the adherent oxide layer and foreign impurities, if any.[43] The fine polishing was done by using 1 μm diamond suspension, and then washed with alcohol followed by air drying. The scanning electron microscope (SEM, Hitachi-S4300 and JEOL JXA-8500F) was used to observe the top down surface morphology of Cu and Cu-W filled TSVs. The composition of Cu-W was measured by electron probe X-ray micro-analyzer (EPMA, JEOL JXA-8500F). For, extrusion measurements, Cu and Cu-W filled TSVs were annealed for 30 minutes at 723 K (450 °C) in a vacuum of 10^{-5} Torr. The extrusion behavior was further assessed with annealing time ranging from 30 to 120 minutes at 723 K (450 °C). The quantitative extrusion heights were measured using a 3D surface profilometer (Nano 3D A&I, Korea) and atomic force microscope (AFM, XE-100).

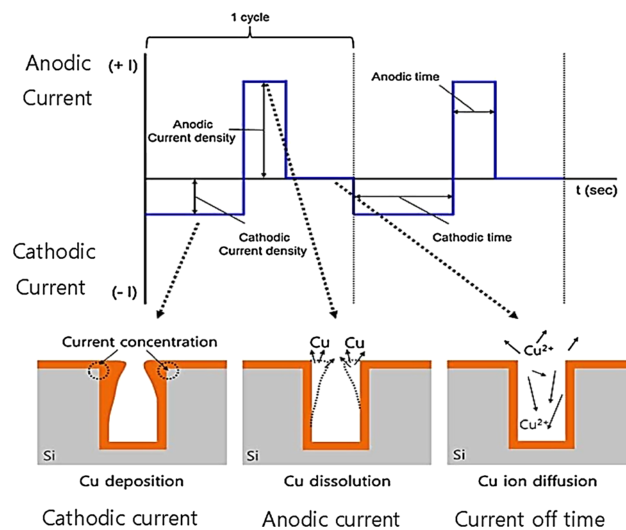

Fig. 2—A schematic of the PPR waveform used for TSV filling depicting different processes occurring in TSV during the cathodic, anodic and current off time.

III. RESULTS AND DISCUSSION

A. *Electroplating of Cu and Cu-W*

The Cu and Cu-W alloy were filled in the TSVs by electroplating. The amount of W in the Cu-W alloy was

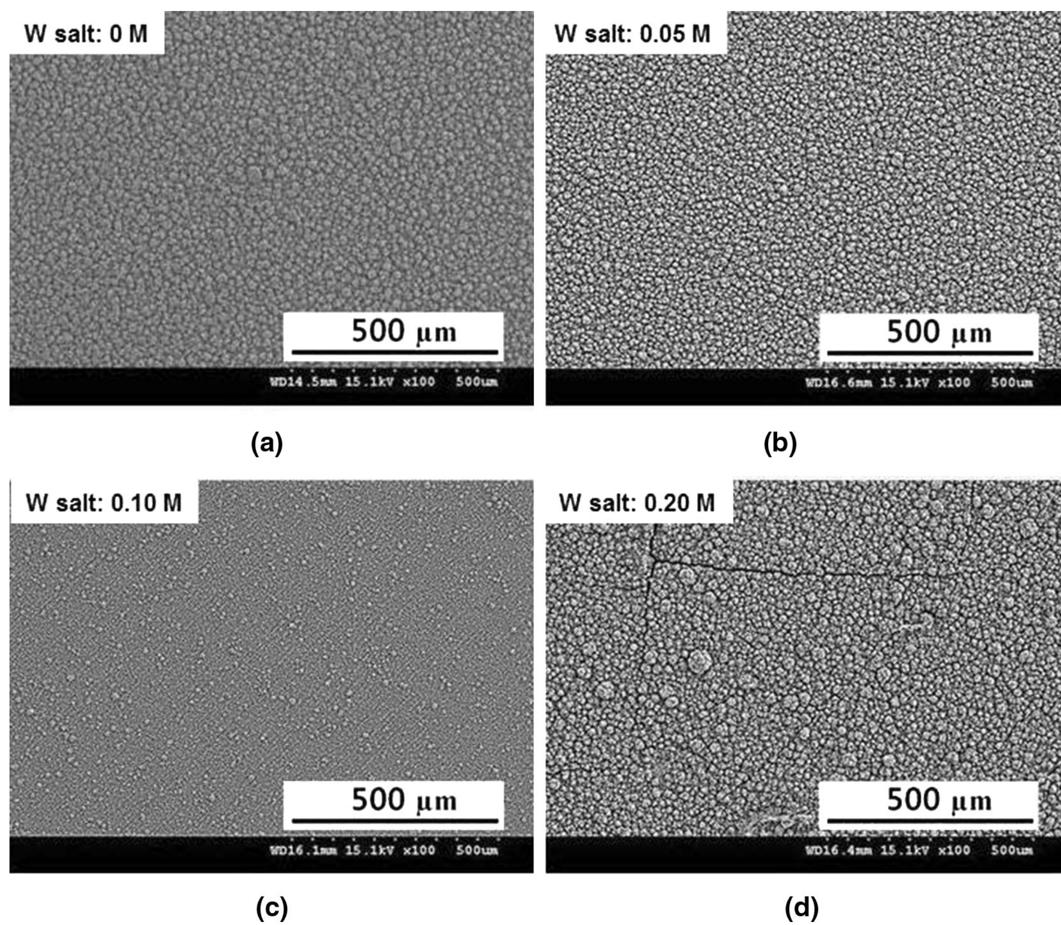

Fig. 3—Morphology of electrodeposited Cu-W coatings as a function of W salt concentration: (*a*) 0 M, (*b*) 0.05 M, (*c*) 0.1 M, and (*d*) 0.2 M.

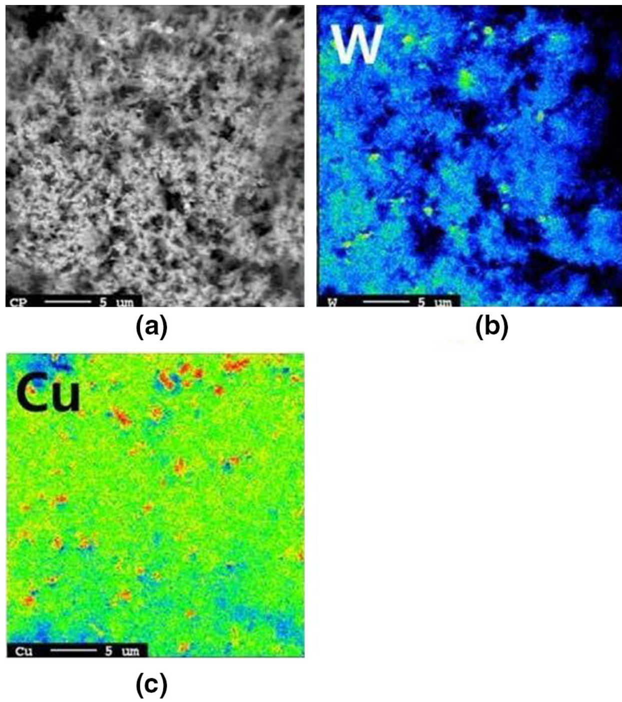

Fig. 4—EPMA analysis of the Cu-W coated layers: (*a*) Secondary electron image of Cu-W coating, (*b*) W map, and (*c*) Cu map. The W salt concentration is 0.1 M.

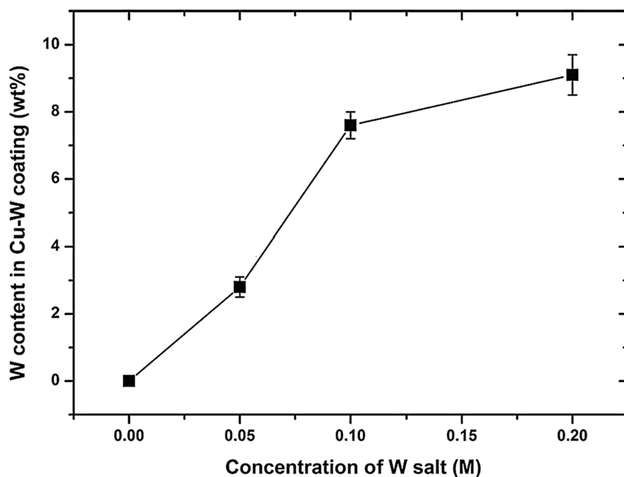

Fig. 5—The amount of W (weight percent) in the Cu-W coating as a function of W salt concentration.

optimized by varying the W salt ($Na_2WO_42H_2O$) concentration. The morphology of the Cu and Cu-W deposits obtained are shown in Figure 3. There is a slight change in morphology of Cu-W alloy deposit up to 0.1 M concentration of W salt. However, a higher concentration of W salt caused the pore formation in the deposits. The best morphology of the Cu-W alloy was obtained at 0.1 M of W salt.

The composition of Cu-W layer was further quantified by the EPMA analysis as shown in Figure 4. The amount of W in the deposits was plotted as a function of W salt in the plating bath (Figure 5). It was noticed that the content of W in the deposit was increased continuously with W salt. The content of W in the deposit was around 7.6 wt pct W at 0.1 M of W salt which reached to a maximum (~9.1 wt pct W) at 0.2 M of W salt. Though the content of W is higher at 0.2 M of W salt yet cracks and pores were found in the microstructure (Figure 3d). It is already known that a higher amount of the reinforcement materials in the electrodeposited metals may cause the pore and crack formation and degrade the deposit properties.[44–46] Therefore, the 7.6 wt pct W in Cu was chosen as a candidate alloy for further extrusion studies.

B. *Cu and Cu-W Filled TSV Characterization*

Figure 6 shows the cross-sectional SEM images of (a) Cu-filled TSV and (b) Cu-W-filled TSV. The EPMA images of Cu-W-filled TSV are also shown in Figure 6(c). It was found that the Cu and Cu-W fillings in TSV were complete and defectless. It indicated an excellent bonding of Cu and Cu-W layer to silicon wafer. The EPMA result as shown in Figure 6(c), illustrates a uniform distribution of W in Cu throughout the *via*. The CTE of the Cu-W layer was determined using Shapery's equation,[47] and was found to be 10.8×10^{-6}/°C, which is significantly smaller than that of pure copper (~16.5×10^{-6}/°C).

C. *Extrusion Characterization*

1. *As deposited samples*

The top down SEM images of Cu and Cu-W filled TSVs are shown in Figure 7. It was observed that no serious defects such as pores, voids, cracks/delamination, *etc*., are present in both of Cu and Cu-W filled TSVs. Such defects are highly undesirable for TSV packaging and may result in the complete failure of the TSV.

Figure 8 illustrates 3D surface images and the corresponding top down surface profile of (a) Cu filed TSV and (b) Cu-W filled TSV. From the depth profiles, the extruded heights of the Cu and Cu-W layer were measured. It was observed that the extruded heights of Cu and Cu-W were −0.275 and −0.720 μm, respectively. The negative values arise from the difference of hardness of Si wafer which is around 10 times harder than Cu or Cu-W phases.[48,49] The relatively soft Cu and Cu-W layer was polished away easily compared to the hard Si wafer.

2. *Annealed samples*

The top down SEM images of (a) Cu-filled TSV and (b) Cu-W filled TSV which were annealed for 30 minutes at 723 K (450 °C) are shown in Figure 9. It was noticed that after annealing, the surface of Cu and Cu-W layer became irregular compared to the surface before annealing (Figure 7). However, signs of cracks and voids were noticed on the surface of the Cu-filled TSV. This type of deformation is widely known as delamination failure. Delamination occurs due to the plastic deformation of Cu layer surrounding the silicon substrate. This is mainly caused by the significant

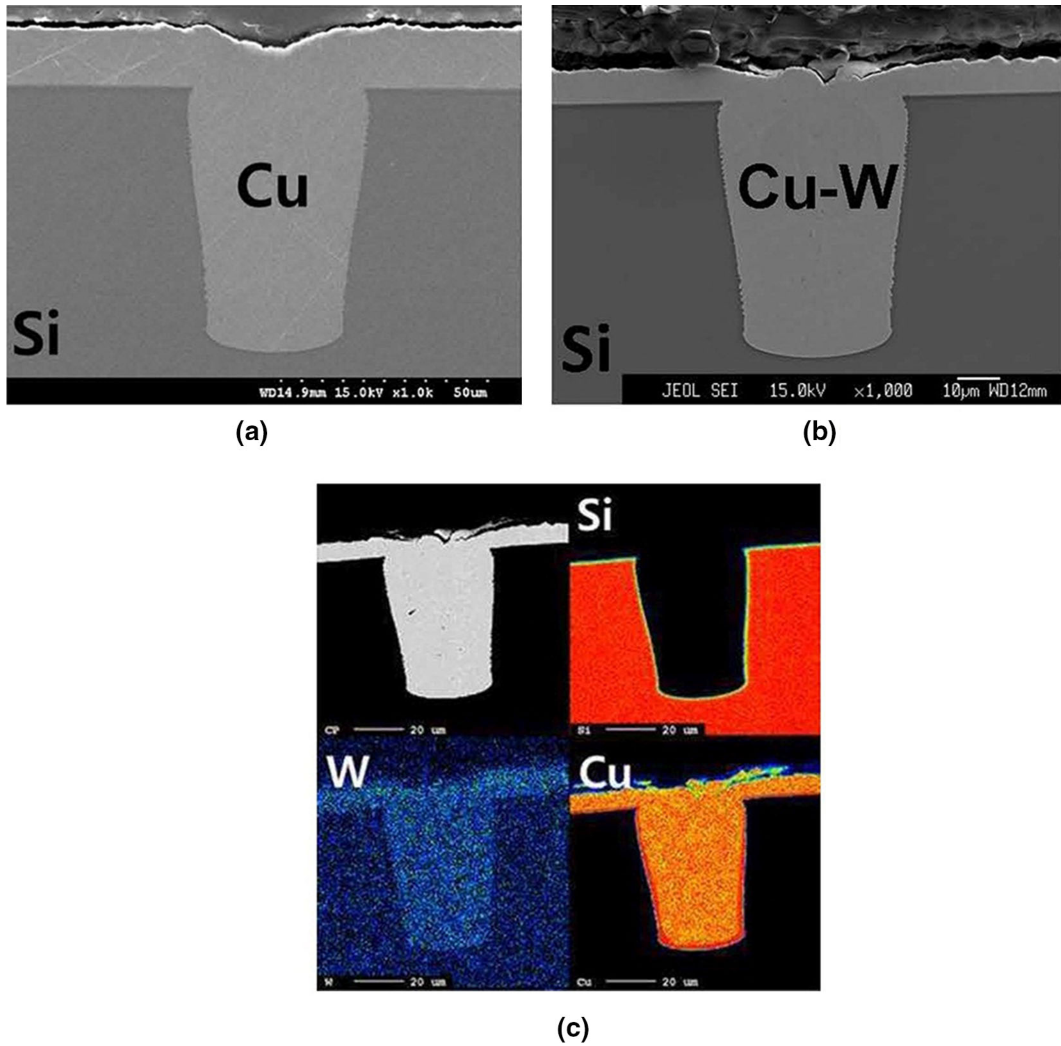

Fig. 6—Cross section SEM images of (*a*) Cu-filled TSV, (*b*) Cu-W-filled TSV, and (*c*) EPMA analysis of Cu-W filled TSV showing a uniform distribution of Win Cu layer.

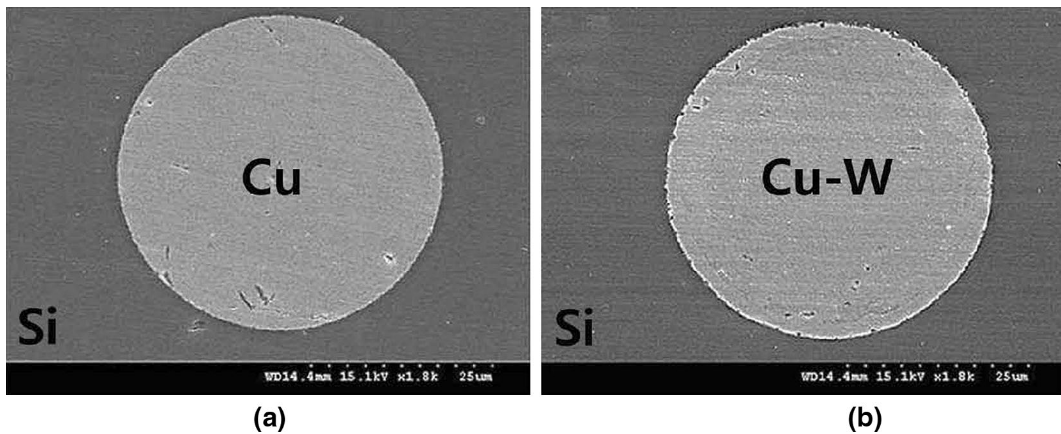

Fig. 7—Top down SEM images of (*a*) Cu-filled TSV and (*b*) Cu-W filled TSV (before annealing).

difference in CTEs between Cu and Si substrate. The plastic strain dominates even after the metal is cooled down to room temperature resulting in the extrusion between Cu and Si interface as shown in Figure 9(a). On the contrary, there was no appreciable delamination between Cu-W and Si as shown in Figure 9(b).

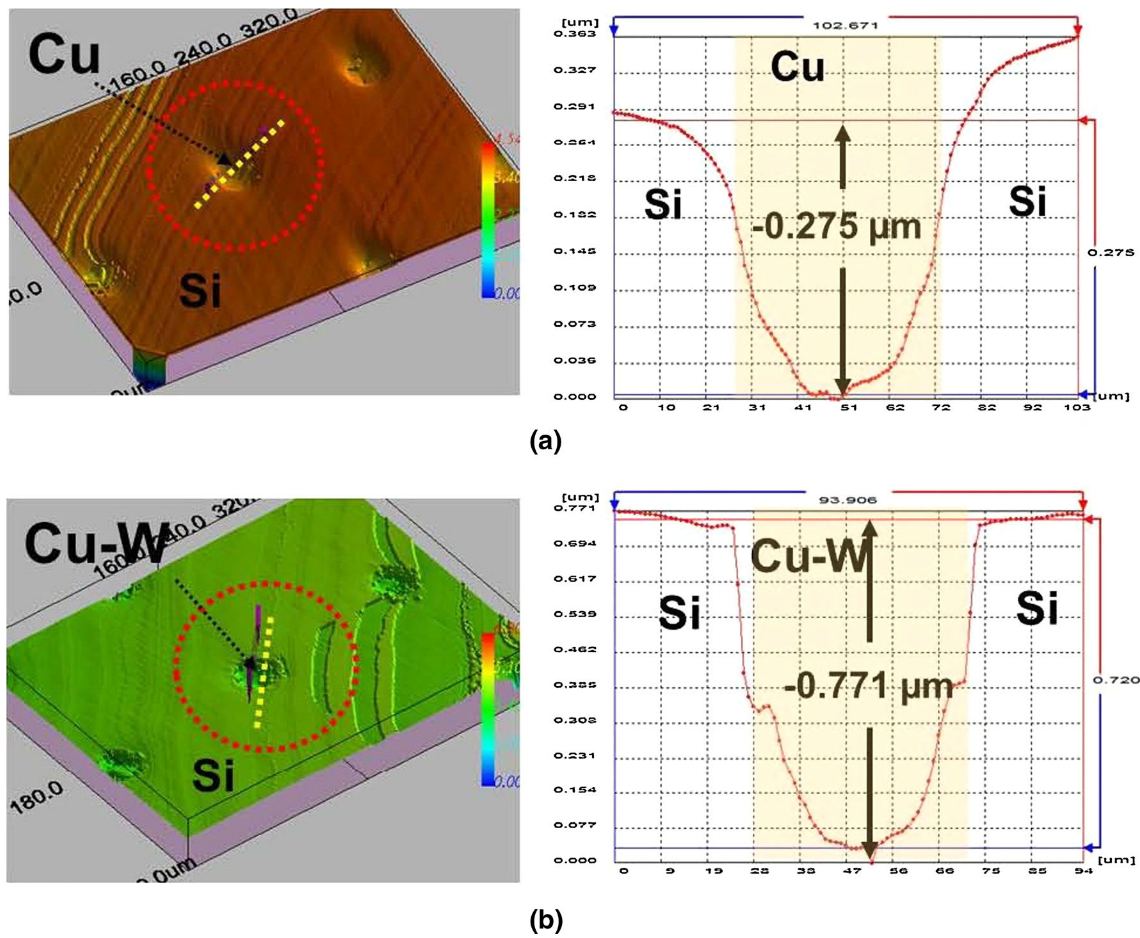

Fig. 8—3D surface images and the corresponding depth profiles of (*a*) Cu-filled TSV and (*b*) Cu-W filled TSV before annealing.

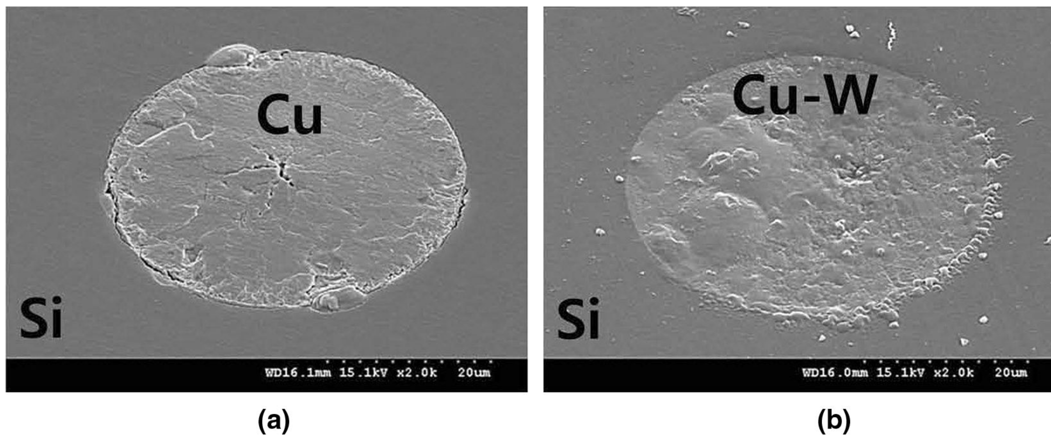

Fig. 9—Top down SEM images of (*a*) Cu-filled TSV and (*b*) Cu-W filled TSV after annealing for 30 min at 723 K (450 °C).

Figure 10 presents the top down 3D surface images and the corresponding depth profiles of Cu and Cu-W filled TSV after annealing. A significant amount of extrusion was observed in Cu-filled TSV as compared to Cu-W filled TSV. This result is in agreement with the SEM micrographs obtained in Figure 9. The extrusion heights of Cu and Cu-W filled TSV were 1.089 and -0.306 μm, respectively. A comparison of Figures 8 and 10 indicated an effective change in extrusion heights of Cu and Cu-W filled TSV before and after annealing, which were found to be 1.369 and 0.465 μm, respectively. This indicated a significant suppression (around 34 pct) of extrusion height of Cu-W filled TSV compared to that of Cu-filled TSV.

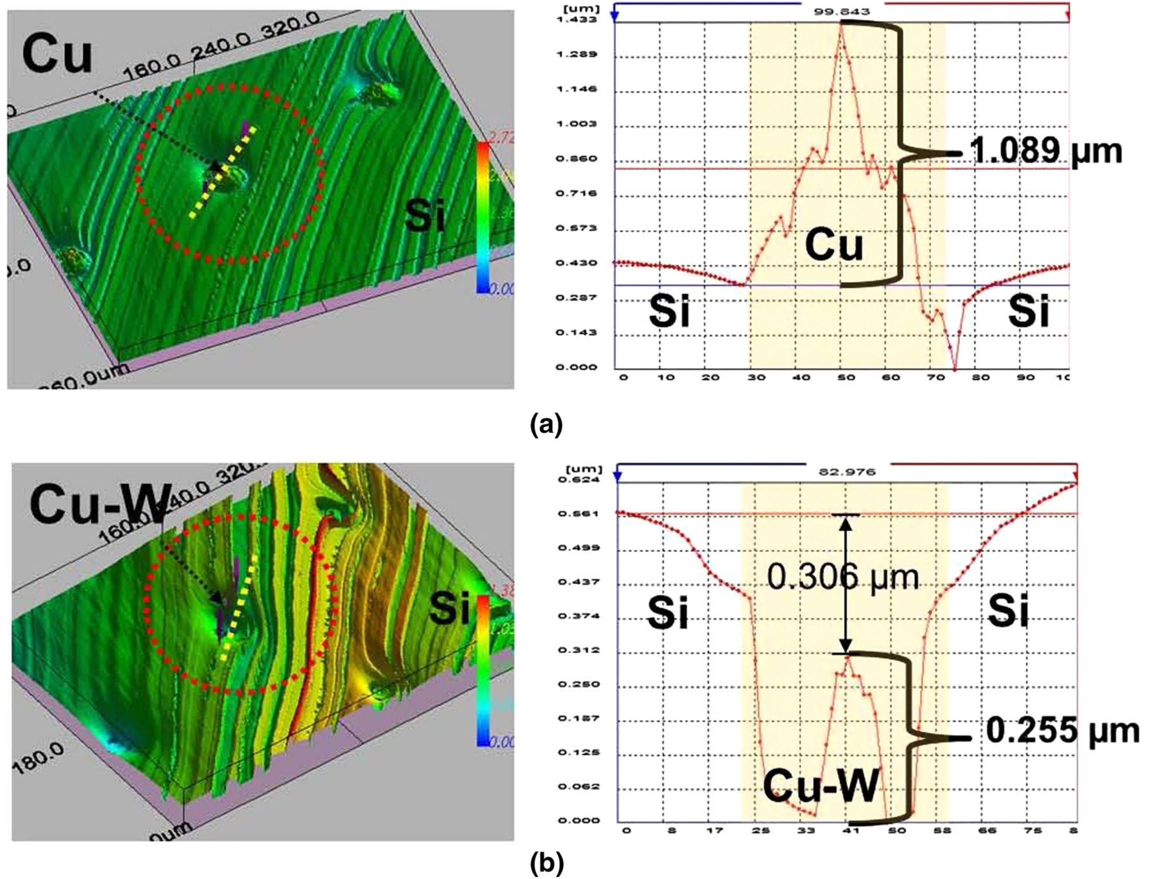

Fig. 10—3D surface images and the corresponding depth profiles of (*a*) Cu-filled TSV and (*b*) Cu-W filled TSV *via* after annealing for 30 min at 723 K (450 °C).

3. *Extrusion kinetics with annealing time*

Figure 11 shows the AFM images of Cu-W filled TSV extrusion height at 723 K (450 °C) for different annealing times varying from 30 to 120 minutes. The change in extrusion height of Cu-filled TSV was not measured since there had already been several reports on the extrusion measurements of Cu-filled TSV.[49–51] The AFM images show that the Cu-W *via* extrusion heights (*i.e.*, *Z* axis) increased continuously with annealing durations up to 120 minutes. To describe the effect of annealing duration on extrusion behavior of Cu-W alloy, the measured extrusion heights were plotted with annealing time.

Figure 12 shows the measured extrusion heights of Cu-W alloy under different annealing durations. The extrusion height of the Cu-filled TSV after annealing at 723 K (450 °C) for 120 minutes was 2.846 μm (solid rectangular symbol in Figure 12), which showed a higher value than that of the Cu-W filled TSV. The extrusion height for Cu-W alloys is 1.254 μm showing 44 pct reduction in Cu-W *via* extrusion height compared to that of Cu-filled TSV. An increase in the extrusion height with annealing duration indicates a grain growth of the Cu-W alloy. The grain size becomes larger with annealing time making it much softer. Soft Cu and a long annealing time lead to a larger plastic and creep deformation. However, in Cu-W alloy, the annealing temperature was not high enough to cause any creep deformation. Thus, extrusion in Cu-W alloy was suppressed considerably as compared to Cu.

The control of annealing duration is also important to restrict the extrusion of TSVs. The stress at annealing temperature slightly decreases with increasing annealing duration because of the stress relaxation effect. The stress at room temperature slightly increases with increasing annealing duration because of severe irreversible deformation. The increase of extrusion heights up to 120 minutes indicated a decrease in the recrystallization temperature by a longer annealing duration and the stress relief mechanism resulted in copper extrusion.[52] A detailed mechanism of extrusion suppression for Cu-W filled TSV will be discussed in the following section.

4. *Extrusion and mechanism of extrusion suppression*

To understand the mechanism of extrusion and extrusion suppression, let us consider Figure 13 showing stress evolution and the grain growth during annealing process of pure copper. It is well known that Cu extrusion is created to relieve internal stresses during annealing.[53] As shown in Figure 13, the filling metal (Cu) passes through three steps during annealing: (1) recovery, (2) recrystallization, and (3) grain growth. During recovery step, with temperature increase

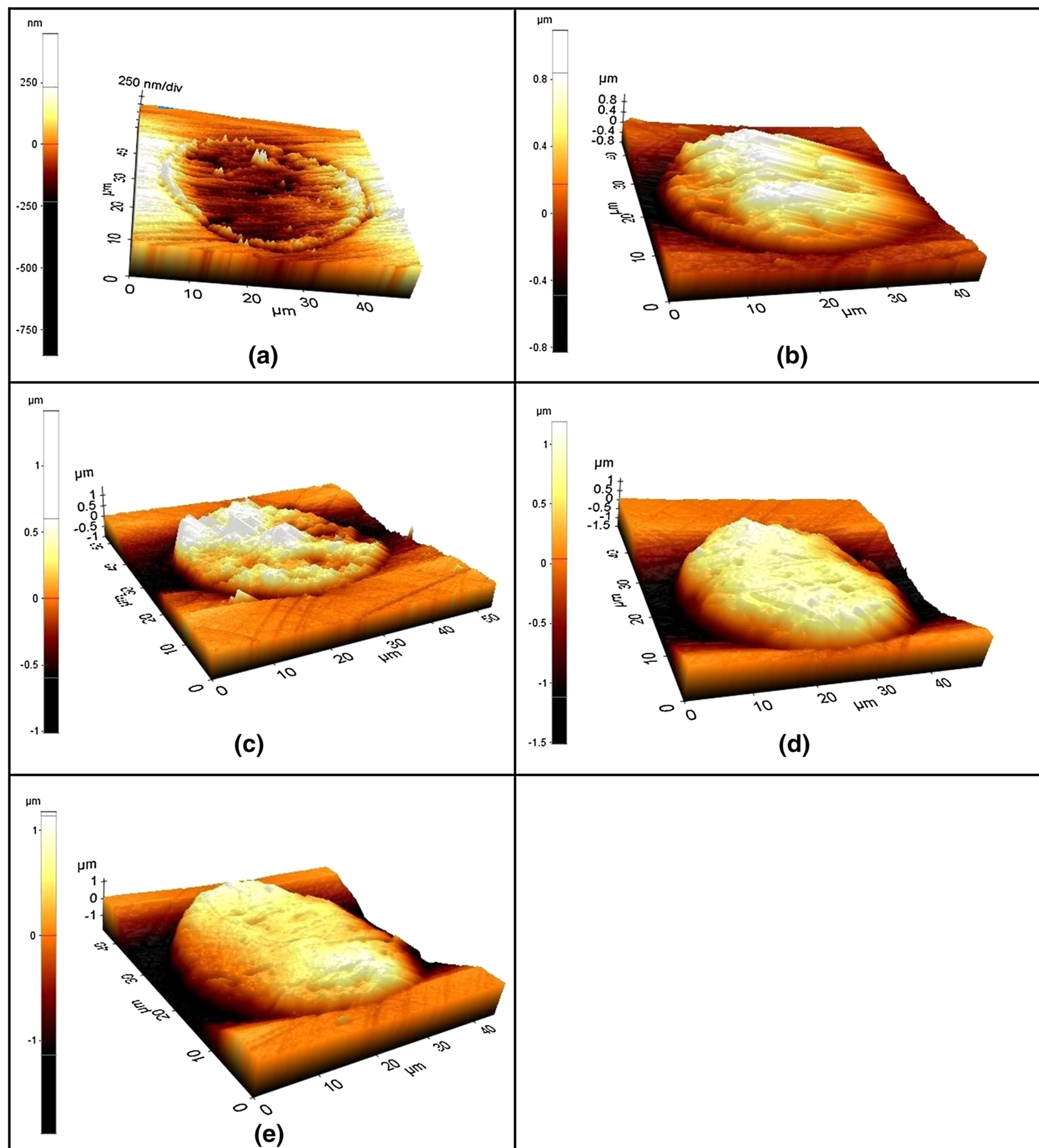

Fig. 11—AFM images of extruded Cu-W filled TSV at various annealing durations (*a*) 30 min, (*b*) 60 min, (*c*) 90 min, (*d*) 120 min, and (*e*) AFM image of extruded Cu-filled TSV annealed for 120 min.

significant amount of internal stresses are relieved until recrystallization temperature (T_R) is reached. The dislocations are moved to grain boundary and get rearranged in minimum energy state; however, the microstructure does not change. In second step, when the annealing temperature exceeds the recrystallization temperature (T_R), new grains of Cu are nucleated by recrystallization process and grain growth begins. The driving force for recrystallization is supplied by a reduction in free volume energy due to the decrease in dislocation density. The recrystallization temperature of Cu is round 423 K to 523 K (150 °C to 250 °C). The internal stresses are relieved continuously during recrystallization process. During final step, with continuous increase in temperature, the newly formed grains grow in size. As the grain growth take place, the mechanical properties of Cu like ductility and hardness are changed. The change in grain size and ductility of Cu which depend on annealing temperature are shown in Figure 13.[53] As discussed in Section III–C–3, the annealing time also raises the grain size at a fixed annealing temperature, where the recrystallization temperature decreases and after stress relief mechanism the extrusion increases.[52]

However, for a film/substrate interaction like a Cu-filled TSV, the annealing behavior is rather different. The geometry of the TSV and CTE mismatch in the filling metal layer (Cu) and the surrounding Si substrate influence significantly the annealing behavior and may result in extrusion defects. This demonstrates that

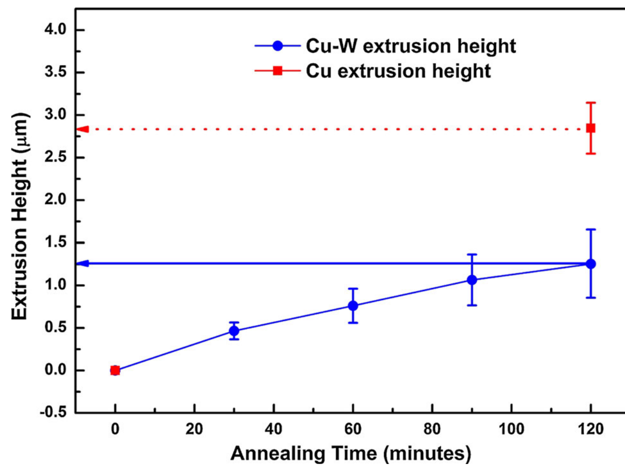

Fig. 12—AFM measurement results of extruded heights of Cu-W filled TSV with increasing annealing duration compared with Cu-filled TSV extrusion.

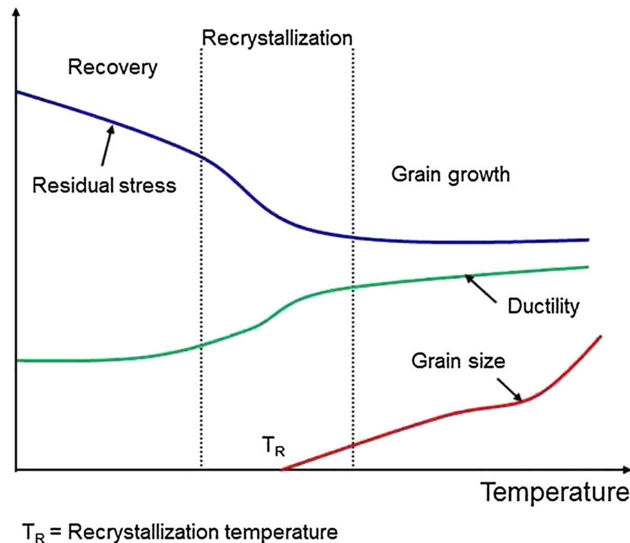

Fig. 13—Stress evolution and grain growth during annealing[53].

annealing of a metal (Cu) filled TSV can give rise to additional stresses at the interface of TSV as compared to the annealing of a pure metal (Cu).

Figure 14 illustrates the various types of thermal stresses that can arise with temperature increase in a Cu-filled TSV. The internal stresses are recovered during recovery from room temperature to 423 K (150 °C). At this stage, there is almost no thermal deformation of Cu layer. When temperature exceeds 423 K (150 °C), in recrystallization stage from 423 K to 523 K (150 °C to 250 °C), thermal stresses are generated and Cu layer deforms due to the presence of surrounding Si substrate. The CTE mismatch in Cu layer and Si substrate causes plastic strains, which remain irreversible even after cooling while elastic strain disappears. The elasto-plastic thermal deformation takes place according to the following equations.[54]

$$\sigma_{th} = E\alpha(T_2 - T_1) \quad [1]$$

$$\varepsilon_{total} = \varepsilon_{el} + \varepsilon_{pl} = \frac{\sigma_{th}}{E} + \alpha(T_2 - T_1) \quad [2]$$

where, σ_{th} is thermal stress, E is young's modulus, α is CTE, T_1 and T_2 are initial and final temperatures, ε is thermal strain, el and pl signifies elastic and plastic deformation, respectively.

In the final stage, when temperature reaches homologous temperature (~0.4 times of melting point), additional creep deformation of Cu layer occurs along with elasto-plastic thermal deformation. The creep strain can be defined according to the following equation.[55]

$$\varepsilon_{cr} = A\exp\left(-\frac{Q}{RT}\right)\sigma_{th}^{n}Y^{n}t^{m} \quad [3]$$

where, ε_{cr} is creep strain, A is constant, Q is activation energy, R is gas constant, T is evaluated temperature, σ_{th} thermal stress, t is time, n and m are stress- and time-hardening exponent. Thus, total strain rate at evaluated temperature considering the effect of creep is as follows.

$$\varepsilon_{total} = \varepsilon_{el} + \varepsilon_{pl} + \varepsilon_{cr} \quad [4]$$

According to Che *et al.*, the constants in Eq. [3] *e.g.*, A, Q, n and m are given by 1.43 × 1010, 197000, 2.5, and −0.9 respectively.[55] Substituting the constants in Eqs. [3] and [4], the total strain of Cu and Cu-W can be determined as follows.

$$\varepsilon_{Cu} = 0.018 \quad [5]$$

$$\varepsilon_{Cu-W} = 0.009 \quad [6]$$

Here, the values of constants are same for both Cu and Cu-W, assuming similar thermal creep behavior of the Cu and Cu-W alloy. After substituting the total length of the depth of the TSV *via* (*i.e.*, 60 μm), the predicted extrusion heights of Cu and Cu-W filled TSVs (for annealing at 723 K (450 °C) and a dwell of 30 minutes) were found to be 1.08 and 0.54 μm, respectively.

The experimentally observed and theoretically calculated values are shown in Table I. The calculated extrusion heights of Cu and Cu-W according to Eq. [1] and (4) are 1.369 and 0.465 μm, respectively. This shows a difference of about 0.289 μm for Cu-filled TSV, and around 0.075 μm for Cu-W filled TSV in experimentally and theoretically measured values of extrusion heights.

The difference between experimental and theoretically calculated extrusion heights of Cu was much greater as compared to that of the Cu-W layer. This significant difference was probably caused by an additional diffusion term during annealing. According to Heryanto *et al.*, extremely high tensile stresses are generated at the top of *via* in comparison to compressive stresses at the bottom of *via* with increase in temperature.[49] This results in stress imbalance throughout the TSV. The diffusion of Cu atoms to the top of *via* was further accelerated by stress disproportion.

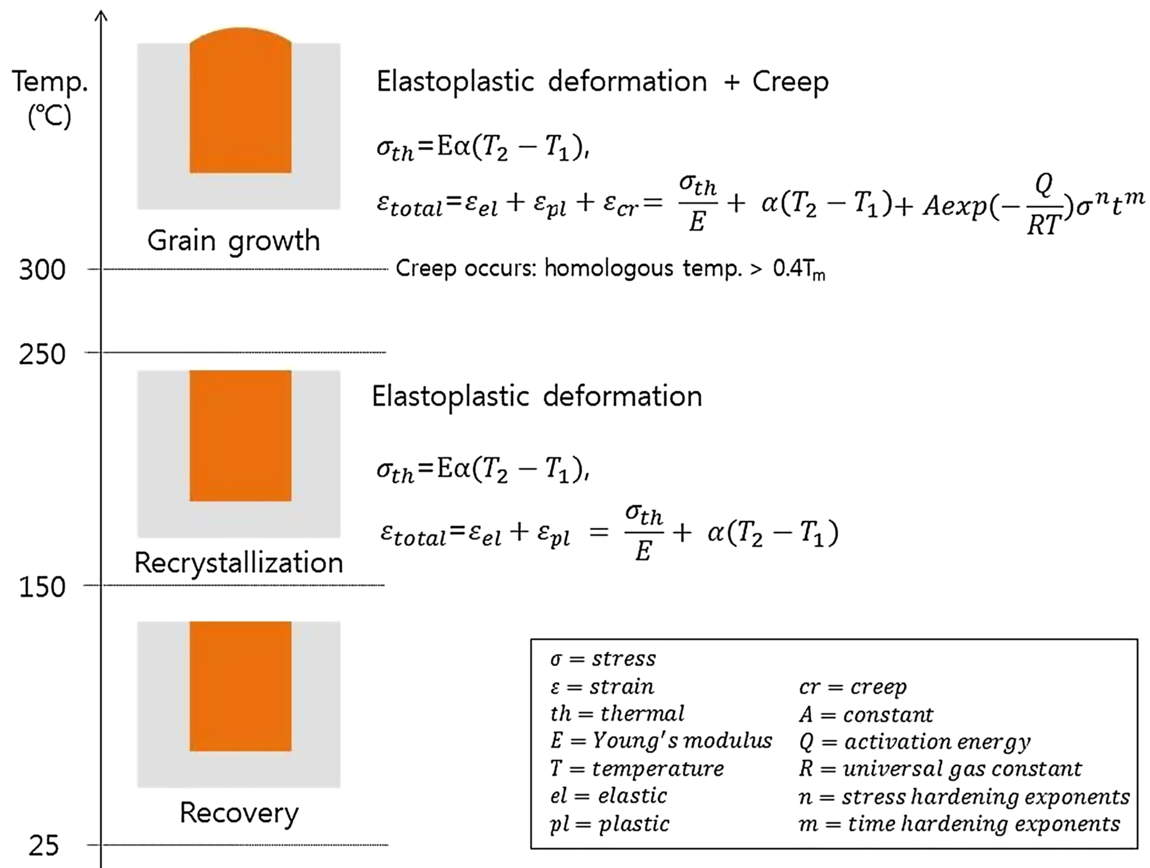

Fig. 14—Schematic of extrusion mechanism during annealing.

Table I. Experimentally Observed and Theoretically Predicted Extrusion Heights of the Cu and Cu-W Filled TSVs After Annealing at 723 K (450 °C) for 30 Min

Sample	Experimental Extrusion Height (μm)	Theoretical Extrusion Height (μm)	Difference (μm)
Cu	1.369	1.08	0.289
Cu-W	0.465	0.54	0.075

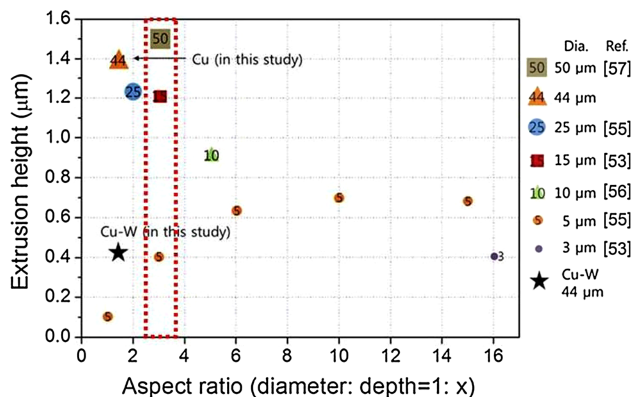

Fig. 15—Cu extrusion heights with respect to *via* diameter and aspect ratio of different TSVs.

Since factor related to diffusion term was omitted in Eq. [4], the extrusion height of Cu measured in the experiment was higher than calculated height. On the other hand, experimental height of Cu-W was almost similar to calculated height. This indicated that the Cu diffusion was likely to be suppressed in presence of W. Tao *et al*. reported that the ability of diffusion prevention was improved by adding 11.89 wt pct of W in NiP, which was used as diffusion barrier layer for Cu and Si.[35] Therefore, it can be concluded that the Cu diffusion during annealing may be suppressed by distributing W in Cu-filled TSV.

The various results of previous reports on extrusion heights of Cu-filled TSV (according to aspect ratio) annealed at 673 K (400 °C) or above are illustrated in Figure 15.[53,55–57] The extrusion result of present study is also presented in Figure 10 for comparison. It is observed that the extrusion height increases from 0.1 to ~0.7 μm as aspect ratio increases from 1:1 to 1:10 under same 5 μm *via* diameter. The extrusion height does not change much when the aspect ratio exceeds 1:10.

In addition, the extrusion height decreases with decreasing the *via* diameter under similar aspect ratio. However, when the *via* diameter is 15 μm or larger, the extrusion heights are mostly above 1.2 μm. In present case, the extrusion height of Cu-W was almost similar in value to that of 5 μm *via* diameter (aspect ratio 1:3) and to with 3 μm *via* diameter (aspect ratio 1:16), compared to extrusion height of Cu with a relatively large 44 μm

via diameter. Consequently, considering other results in Figure 15, it is confirmed that Cu-W filled TSV was effective to suppress the extrusion height of TSV.

IV. CONCLUSIONS

Electrodeposition of Cu-W in TSV has been suggested to suppress the extrusion height of TSV as compared to Cu-filled TSV in this study. The Cu-7.6 wt pctW was selected as filling composition which showed good plating finish. Scanning electron micrographs of top down images of Cu and Cu-W filled TSVs show that there is no crack formation of delamination in Cu-W filled TSV, while in Cu-filled TSV delamination was noticed after annealing for 30 minutes. It was observed that annealing of Cu-W-filled TSV for 30 minutes at 723 K (450 °C), causes reduced extrusion height compared to a Cu-filled TSV (as a reference). From the surface profilometry, the net extrusion of Cu-7.6 pctW and Cu were 0.465 and 1.369 μm, respectively. This result showed that the extrusion in Cu-7.6 pctW was about 34 pct lower as compared to that of Cu-filled TSV, and hence Cu-7.6 pctW was verified to be effective for suppression of extrusion in TSV. When the annealing time was increased, the extrusion height also increased. On increasing the annealing duration from 30 to 120 minutes, Cu-W *via* increased considerably. However, Cu-W alloy still played a role in extrusion suppression as compared to pure copper. Cu-W alloy showed 44 pct reduction in extrusion height as compared to Cu at 723 K (450 °C) for a longer dwell time of 120 minutes. Based on these experimental results, for Cu the diffusion mechanism was elastoplastic and creep diffusion, while for Cu-W filled TSV, the diffusion occurs through only elastoplastic deformation. It is concluded that the mechanism of suppression of extrusion in Cu-W filled TSV is due to the presence of W which suppressed the copper diffusion at high temperature in Cu-W filled TSV.

ACKNOWLEDGMENTS

The authors acknowledge the financial support provided by the Seoul R&BD Program (JP130043), and Business for Cooperative R&D between Industry, Academy and Research Institute funded Korea Small and Medium business Administration (Grants No. C0213709).

REFERENCES

1. M. Motoyoshi: *Proc. IEEE*, 2009, vol. 97, pp. 43–48.
2. Y.-K. Ko, Y.-H. Ko, J.-H. Bang, and C.-W. Lee: *JWJ*, 2014, vol. 32, pp. 19–26.
3. D.-G. Kim, J.-W. Kim, S.-S. Ha, J.-P. Jung, Y.-E. Shin, J.-H. Moon, and S.-B. Jung: *JWJ*, 2006, vol. 24, pp. 172–78.
4. M. Umemoto, K. Tanida, Y. Nemoto, M. Hoshino, K. Kojima, Y. Shirai, and K. Takahashi: *IEEE 54th Electronic Components and Technology Conference*, 2004, vol. 1, pp. 616–23.
5. T. Ritzdorf, L. Graham, S. Jin, C. Mu, and D.B. Fraser: *IEEE International Interconnect Technology Conference*, 1998, vol. 1, p. 166.
6. D.H. Kim, S. Mukhopadhyay, and S.K. Lim: *IEEE International Interconnect Technology Conference*, 2009, p. 26.
7. M.-H. Roh, J.-H. Lee, W.J. Kim, J.P. Jung, and H.-T. Kim: *JWJ*, 2013, vol. 31, pp. 11–16.
8. S.-H. Kee, J.-O. Shin, I.-H. Jung, W.-J. Kim, and J.-P. Jung: *JWJ*, 2014, vol. 32, pp. 11–18.
9. R. Hon, S.W.R. Lee, S.X. Zhang, and C.K. Wong: *IEEE Electronics Packaging Technology Conference*, 2005, pp. 384–89.
10. R. Tummala, J.E.J. Rymasewski, and A.G. Klopfenstein: *Microelectronics Packaging Handbook*, 2nd ed., Chapman & Hall, New York, 1997.
11. J.N. Calata, J.G. Bai, X. Liu, S. Wen, and G.Q. Lu: *IEEE Trans. Adv. Packag.*, 2005, vol. 28, pp. 404–12.
12. A.S. Budiman, H.A.S. Shin, B.J. Kim, S.H. Hwang, H.Y. Son, M.S. Suh, Q.H. Chung, K.Y. Byun, N. Tamura, M. Kunz, and Y.C. Joo: *Microelectron. Reliab.*, 2012, vol. 52, p. 530.
13. X. Liu, Q. Chen, V. Sundaram, R.R. Tummala, and S.K. Sitaraman: *Microelectron. Reliab.*, 2013, vol. 53, pp. 70–78.
14. Y.-K. Ko, Y.-H. Ko, J.-H. Bang, and C.-W. Lee: *JWJ*, 2014, vol. 32, pp. 68–73.
15. T.C. Tsai, W.C. Tsao, W. Lin, C.L. Hsu, C.L. Lin, C.M. Hsu, J.F. Lin, C.C. Huang, and J.Y. Wu: *Microelectron. Eng.*, 2012, vol. 92, pp. 29–33.
16. I.E. Wolf, K. Croes, O.V. Pedreira, R. Labie, A. Redolfi, M.V.D. Peer, K. Nanstreels, C. Okoro, B. Vandevelde, and E. Beyne: *Microelectron. Reliab.*, 2011, vol. 51, pp. 1856–59.
17. S.K. Ryu, T. Jiang, K.H. Lu, J. Im, H.Y. Son, K.Y. Byun, R. Huang, and P.S. Ho: *Appl. Phys. Lett.*, 2012, vol. 12, pp. 041901–04.
18. K.N. Tu, H.-Y. Hsiao, and C. Chen: *Microelectron. Reliab.*, 2013, vol. 53, pp. 2–6.
19. L. Xu, P. Dixit, J. Miao, J.H.L. Pang, X. Zhang, K.N. Tu, and R. Preisser: *Appl. Phys. Lett.*, 2007, vol. 90, pp. 033111–13.
20. N. Lin, J. Miao, and P. Dixit: *Microelectron. Reliab.*, 2013, vol. 53, pp. 1943–53.
21. H.-A.-S. Shin, B.-J. Kim, J.-H. Kim, S.-H. Hwang, A. S. Budiman, H.-Y. Son, K.-Y. Byun, N. Tamura, M. Kunz, D.-I. Kim, and Y.-C. Joo: *J. Electron. Mater.*, 2012, vol. 41, pp. 712–19.
22. D. Xu, W.L. Kwan, K. Chen, X. Zhang, V. Ozolinš, and K.N. Tu: *Appl. Phys. Lett.*, 2007, vol. 91, p. 254105.
23. T. Wang, K. Jeppson, L. Ye, and J. Liu: *Small*, 2011, vol. 7, pp. 2313–17.
24. A.S. Muhsan, F. Ahmad, N.M. Mohamed, and M.R. Raza: *J. Nanoeng. Nanomanuf.*, 2013, vol. 3, pp. 248–52.
25. B. Horvath, J. Kawakita, and T. Chikyow: *Jpn. J. Appl. Phys.*, 2014, vol. 53, p. 06JH01.
26. Y.T. Ding, Y.Y. Yan, Q.W. Chen, S.W. Wang, X. Chen, and Y.Y. Chen: *Sci. China Technol. Sci.*, 2014, vol. 57, pp. 1616–25.
27. R. Sato, A. Tsukada, Y. Sato, Y. Iwata, H. Murata, S. Sekine, R. Kimura, and K. Kishi: *3D Systems Integration Conference*, IEEE, Osaka, 2012, pp. 1–4.
28. C.Y. Ho and R.E. Taylor: *Thermal Expansion of Solids*, ASM International, Materials Park, OH, 1998.
29. H. Kikuchi, Y. Yamada, A.M. Ali, J. Liang. T. Fukushima, T. Tanaka, and M. Koyanagi: *Jpn. J. Appl. Phys.*, 2008, vol. 47, pp. 2801–06.
30. Y. Meng, Y. Shen, C. Chen, Y. Li, and X. Feng: *Appl. Surf. Sci.*, 2013, vol. 282, pp. 757–64.
31. M.A.E. Hadek and S.M. Kaytbay: *Metall. Mater. Trans. A*, 2013, vol. 44A, p. 544.
32. Z. Ghaferi, K. Raeissi, M.A. Golozar, and H. Edris: *Surf. Coat. Technol.*, 2011, vol. 205, p. 497.
33. G.A. Dosovitskiy, S.V. Samoilenkov, A.R. Kaul, and D.P. Rodionov: *Int. J. Thermophys.*, 2009, vol. 30, p. 1931.
34. M. Ahmadi and M.J-F. Guinel: *J. Alloys Compd.*, 2013, vol. 574, pp. 196–205.
35. Y. Tao, A. Hu, T. Hang, L. Peng, and M. Li: *Appl. Surf. Sci.*, 2013, vol. 282, pp. 632–37.
36. K.S. Kim, Y.C. Lee, J.H. Ahn, J.Y. Song, C.D. Yoo, and S.B. Jung: *Korean J. Met. Mater.*, 2010, vol. 48, pp. 1028–34.
37. A. Brenner: *Electrodeposition of Alloys: Principles and Practice*, Academic Press Inc., New York, 1963.

38. I. Mizushima, P.T. Tang, H.N. Hansen, and M.A.J. Somers: *Electrochim. Acta*, 2006, vol. 51, pp. 6128–34.
39. Y.M. Lin and S.C. Yen: *Appl. Surf. Sci.*, 2008, vol. 178, pp. 116–126.
40. V.M. Dublin: *Microelectron. Eng.*, 2003, vol. 70, pp. 461–469.
41. S.C. Hong, W.G. Lee, W.J. Kim, J.H. Kim, and J.P. Jung: *Microelectron. Reliab.*, 2011, vol. 51, pp. 2228–35.
42. M.H. Roh, S.Y. Park, W.J. Kim, and J.-P. Jung: *JWJ*, 2011, vol. 29, pp. 295–300.
43. ASTM E 3-95 1995 *Standard Practice for Preparation of Metallographic Specimens..*
44. Z.-L. Lu, L.-M. Luo, J.-B. Chen, X.-M. Huang, J.-G. Cheng, and Y.-C. Wu: *Mater. Sci. Eng. A*, 2015, vol. 626, pp. 61–66.
45. A. Sharma, S. Bhattacharya, S. Das, and K. Das: *Metall. Mater. Trans. A*, 2013, vol. 44A, pp. 5587–5601.
46. A. Sharma, S. Bhattacharya, S. Das, H.-J. Fecht, and K. Das: *J. Alloys Compd.*, 2013, vol. 574, pp. 609–16.
47. D.K. Shin and J.J. Lee: *IEEE Trans. Compon. Packag. Manuf. Technol. B*, 1998, vol. 21, pp. 413–21.
48. J. Yan, H. Takahashi, J.I. Tamaki, X. Gai, H. Harada, and J. Patten: *Appl. Phys. Lett.*, 2005, vol. 86, p. 181913.
49. A. Heryanto, W.N. Putra, A. Trigg, S. Gao, W.S. Kwon, F.X. Che, X.F. Ang, J. Wei, R.I. Made, C.L. Gan, and K.L. Pey: *J. Electron. Mater.*, 2012, vol. 41, pp. 2533–42.
50. I.D. Wolf, K. Croes, O.V. Pedreira, R. Labie, A. Redolfi, and M.V. Peer: *Microelectron. Reliab.*, 2011, vol. 51, pp. 1856–59.
51. L.W. Kong, A.C. Rudack, P. Krueger, E. Zschech, S. Arkalgud, and A.C. Diebold: *Microelectron. Eng.*, 2012, vol. 92, pp. 24–28.
52. D. Askeland, P.P. Fulay, and W. Wright: *The Science and Engineering of Materials,* 6th ed., Cengage Learning, Stamford, CT, 2010.
53. P. Saettler, M. Boettcher, and K.J. Wolter: *IEEE Electronic Components and Technology Conference*, San Diego, CA, 2012, pp. 619–24.
54. R.L. Web and N.H. Kim: *Principles of Enhanced Heat Transfer*, 2nd ed., Wiley, New York.
55. F.X. Che, W.N. Putra, A. Heryanto, A. Trigg, X. Zhang, and C.L. Gan: *IEEE Trans. Compon. Packag. Manuf. Technol.*, 2013, vol. 3, pp. 732–39.
56. D. Zhang, K. Hummler, L. Smith, and J.J.Q. Lu: *IEEE Electronic Components and Packaging Conference*, Las Vegas, NV, 2013, pp. 1407–13.
57. D. Malta, C. Gregory, M. Lueck, D. Temple, M. Krause, F. Altmann, M. Petzold, M. Weatherspoon, and J. Miller: *IEEE Electronic Components and Technology Conference*, Lake Buena Vista, FL, 2011, pp. 1815–21.